University of Bremen
Institute of Environmental Physics (IUP)

Constraining uncertainties in multi-model projections of future climate with observations

Dissertation

Author:
Manuel Schlund

Supervisors:
Prof. Dr. Veronika Eyring
Prof. Dr. Pierre Gentine

This thesis is submitted for the degree
Doktor der Naturwissenschaften (Dr. rer. nat.)

March 2021

Abstract (English version)

TBA.

Abstract (German version)

TBA.

Contents

List of Figures

List of Tables

1. Introduction

1.1. Motivation

- Why is climate change relevant for the society?
  - Cite latest warming reports, also other variables (droughts, extreme events, etc.)
  - basic physics of greenhouse gases (vibration modes, etc.)
  - definition of radiative forcing
  - well-mixed greenhouse gases (water vapor, CO2, CH4) + sources
  - long-lived vs. short-lived GHGs?
  - aerosols + cooling effect
  - natural vs. anthropogenic effects (D & A) -> clear evidence that climate change over 21st century is caused by human influence (https://globalwarmingindex.org/, Haustein et al., 2017)

1.2. Structure of the Thesis

Parts of this thesis are published in multiple peer-reviewed publications (two first-author studies and six co-author studies). If applicable, this is clearly stated at the beginning of each chapter. Chapter 2 introduces the scientific background for this thesis. This includes relevant literature that is used as a baseline for this thesis. Chapter 3 gives an overview over the contributions made to the Earth System Model Evaluation Tool (ESMValTool), an open-source software for the analysis of ESMs. These contributions helped improving the routine evaluation of ESMs which is useful for the whole scientific community and lead to co-authorship in four peer-reviewed studies (Eyring et al., 2020; Lauer et al., 2020; Righi et al., 2020; Weigel et al., 2020). Chapter 4 covers the assessment of policy-relevant climate metrics like the Effective Climate Sensitivity (ECS) and the Transient Climate Response (TCR) in the latest generation of ESMs. This work is already published in two scientific publications (Bock et al., 2020; Meehl et al., 2020). Since the ECS and TCR are considerably higher in this

new climate model generation, chapter 5 describes the assessment of emergent constraints (a technique to reduce uncertainties in climate model projections, see section 2.4 on page 19) on the ECS for these ESMs. The contents of this chapter are published in *Earth System Dynamics* (Schlund, Lauer, et al., 2020). Chapter 6 focuses on a new method to reduce climate model uncertainties based on Machine Learning (ML). As an example, the method is applied to the photosynthesis rate at the end of the 21st century, which is already published in the *Journal of Geophysical Research: Biogeosciences* (Schlund, Eyring, et al., 2020). Finally, chapter 7 provides a summary of the results of this thesis and gives an outlook of possible future works.

2. Scientific Background

This chapter introduces the scientific background of this thesis. First, basic concepts of climate model simulations and associated uncertainties are introduced. Next, the fundamental biogeochemical processes of the global carbon cycle and important metrics describing climate change are presented. Finally, state-of-the art techniques used reduce uncertainties in projections of the future climate are shown. These methods form the basis for the new techniques developed in this thesis.

2.1. Earth System Models: Simulations and Analysis

2.1.1. Numerical Climate Modeling

In contrast to other fields of science, researching the future evolution of the Earth's climate cannot be purely done by performing experiments in a laboratory. Due to the immense complexity of the Earth system (including physical, biological and chemical processes on various temporal and spatial scales and their mutual interactions), we do not have access to a tiny replica of the Earth that we can analyze when exposed to different external conditions (Flato, 2011). While observing the current state of the Earth System is (relatively) straightforward, gaining evidence about the future evolution of the climate by only considering present-day observations is rather difficult.

A possible way out is given by numerical climate models, which offer the possibility to simulate the Earth's climate on a computer. The first numerical climate models came up in the 1960s and were based on weather prediction models (Flato, 2011). Early models from the 1970s simulated only the physical components of the climate system: atmosphere, land surface, ocean and sea ice (see figure 2.1). The basis of these so-called Atmosphere-Ocean General Circulation Models (AOGCMs) (Flato et al., 2013) is the numerical solving of the differential equations describing the exchange of energy and matter between these physical components.

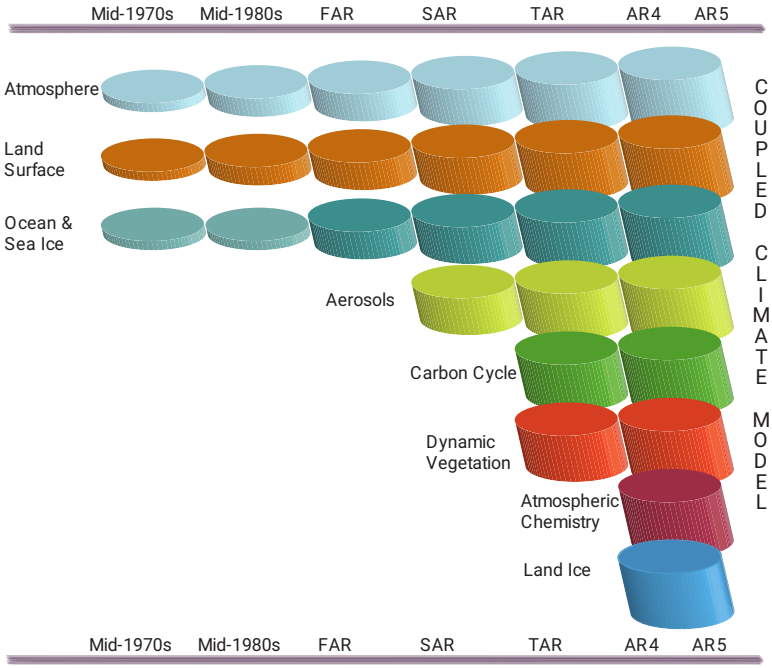

Figure 2.1.: Historical evolution of coupled climate models over the last 45 years. In early days, these models were so-called Atmosphere-Ocean General Circulation Models (AOGCMs) and only included three components: the atmosphere, the land surface and the ocean. Over the time, the individual components grew in complexity and included a wider range of processes (illustrated by the growing cylinders). Eventually, more and more components (aerosols, carbon cycle, etc.) were added to the coupled system, forming the modern Earth System Models (ESMs). Taken from Cubasch et al. (2013).

Over the course of the years, climate models became more and more complex by including a wider range of processes within the components, but also by introducing new components to the coupled system. Examples of these are aerosols, the carbon cycle, a dynamic vegetation, atmospheric chemistry and land ice (see figure 2.1). AOGCMs coupled to these additional components are called Earth System Models (ESMs), which are the current state-of-the-art models that allow the most sophisticated simulations of the Earth's climate. In contrast to AOGCMs, ESMs enable the simulation of biological and chemical processes in addition to the dynamics of the physical components of the Earth system. Especially in the context of anthropogenic climate change, these additional processes are of uttermost importance for realistic climate model simulations, since the anthropogenic interference with the Earth system directly influences the various biogeochemical cycles of the Earth. For example, the emission of the most prominent Greenhouse Gas (GHG), carbon dioxide (CO_2), immediately

impacts the global carbon cycle by inserting additional carbon into the system (for details see section 2.3). Further examples include land use changes like the deforestation of tropical rainforests, which also directly influences several biogeochemical cycles (e.g. carbon cycle, nitrogen cycle, phosphorus cycle, etc.) by altering respective sinks and sources.

Due to the complex interactions between the different components of the Earth system, these changes in the biogeochemical processes also affect the physical properties of the climate system. For example, due to the global carbon cycle, only about 50 % of the emitted CO_2 by humankind remains in the atmosphere (Friedlingstein et al., 2019). The residual part is absorbed by the two other main carbon sinks of the planet, the terrestrial biosphere and the ocean. Since only atmospheric CO_2 can act as GHG by introducing an additional radiative forcing to the Earth System leading to increasing surface temperatures, this uptake of CO_2 by the carbon cycle slows down global warming.

2.1.2. CMIP

Due to the complex nature of the Earth system itself, numerical models of it consist of hundreds of thousands of lines of computer code. Thus, a standardization to a certain degree is crucial for the various research groups developing ESMs all around the world in order to obtain comparable output and to facilitate model analysis. For this reason, the Working Group on Coupled Modelling (WGCM) of the World Climate Research Programme (WCRP) initiated the Coupled Model Intercomparison Project (CMIP) in 1995, with the objective to "better understand past, present and future climate changes arising from natural, unforced variability or in response to changes in radiative forcing in a multi-model context" (WCRP, 2020). One major element of CMIP is to establish common standards, coordination, infrastructure, and documentation in order to facilitate the distribution of climate model output (Eyring et al., 2016).

A further main aspect is to provide a set of standardized experiments for global climate model simulations. To participate in the latest phase of CMIP, CMIP6, climate models need to run a *historical* simulation of the period 1850–2014 and the so-called Diagnostic, Evaluation, and Characterisation of Klima (DECK) experiments, which include a pre-industrial control run (*piControl*), a historical Atmospheric Model Intercomparison Project (MIP) simulation (*amip*), a simulation forced with an abrupt quadrupling of CO_2 (*abrupt-4xCO2*) and a simulation forced with a 1 % per year increase of the atmospheric CO_2 concentration

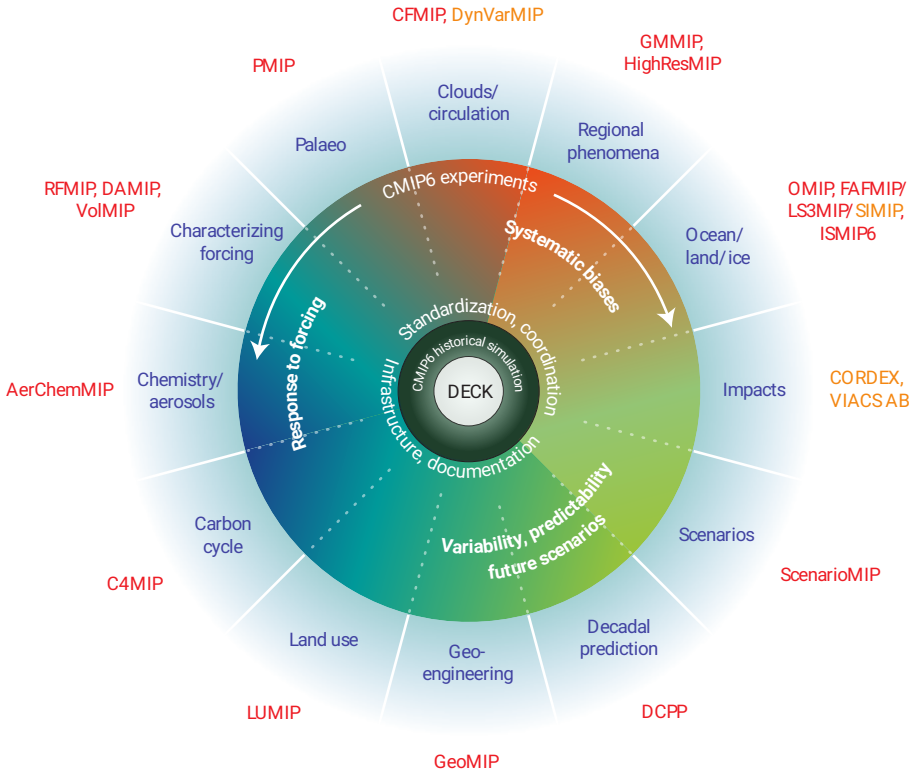

Figure 2.2.: Schematic of the experiment design of Phase 6 of the Coupled Model Intercomparison Project (CMIP6). The center of the circle illustrates the four DECK (Diagnostic, Evaluation, and Characterisation of Klima) experiments and the CMIP6 historical simulation. The circular sectors show additional science themes that can be explored through the 21 CMIP6-Endorsed Model Intercomparison Projects (MIPs). Taken from Simpkins (2017).

(*1pctCO2*) (Eyring et al., 2016). This is shown in the center of figure 2.2, which illustrates the experimental design of CMIP6.

To increase diversity and answer more scientific questions, CMIP6 models can participate in the so-called CMIP6-Endorsed MIPs, of which CMIP6 offers 21 (see circular sectors in figure 2.2). Some MIPs offer additional experiments to explore specific aspects of the Earth system, like the Coupled Climate-Carbon Cycle Model Intercomparison Project (C4MIP) which focuses on the carbon cycle (Jones et al., 2016) or the Aerosol Chemistry Model Intercomparison Project (AerChemMIP) which focuses on aerosol chemistry (W. J. Collins et al., 2017). Other MIPs allow the assessment of future climate change. An example is the Scenario Model Intercomparison Project (ScenarioMIP), which provides common experiments that simulate different possible futures (O'Neill et al., 2016). These experiments are based on the so-called Shared Socioeconomic Pathways (SSPs), a set of alternative pathways of future societal development

(O'Neill et al., 2017; O'Neill et al., 2013). For each experiment, a set of emissions and land use changes is calculated from the SSPs (Riahi et al., 2017) which are then used to force the global climate models. For ScenarioMIP, five different SSPs are considered, ranging from SSP1 (sustainability) to SSP5 (fossil-fuel development). Each SSP is combined with a climate outcome (measured as radiative forcing in the year 2100) based on a particular forcing pathway that Integrated Assessment Modelss (IAMs) have shown to be feasible. For example, SSP5-8.5 represents a scenario based on a fossil-fuel development with a radiative forcing of 8.5 Wm^{-2} in 2100 while SSP1-2.6 represents a sustainable future with a radiative forcing of 2.6 Wm^{-2} in the year 2100. The two other main scenarios (called *Tier 1* experiments in ScenarioMIP) are the SSP2-4.5 and SSP3-7.0 scenarios. In contrast to the ScenarioMIP experiments, the corresponding CMIP5 counterparts (Taylor et al., 2012), the so-called Representative Concentration Pathways (RCPs), only used the radiative forcing in 2100 as only dimension to describe the possible futures (e.g. RCP8.5, RCP4.5, RCP2.6, etc.).

In this thesis, climate model data from the two most recent CMIP generations is used, CMIP5 and CMIP6. More detailed information about the specific variables and experiments analyzed is given in the corresponding chapters.

2.1.3. Sources of Uncertainties in Climate Model Projections

Simulations from climate model ensembles of CMIP allow us to assess the impact of future climate change in a consistent and transparent way. Especially the ScenarioMIP experiments can give valuable insights into the upcoming development of the Earth system by providing *projections* of the future climate. In contrast to climate predictions, climate projections run over multiple decades and depend upon the future scenario considered, which are based on assumptions that may or may not turn out to be correct. On the contrary, climate predictions are attempts to predict the actual evolution of the climate on much shorter time scales from seasons to years. Similar to any other scientific experiment, climate model projections suffer from associated uncertainties. There are three major sources of climate model projections we can distinguish: natural variability, climate response uncertainty and emission uncertainty (Hawkins & Sutton, 2009, 2010). Figure 2.3 shows these three sources for the projected global mean surface temperature anomaly over the 21$^{\mathrm{st}}$ century.

Natural variability is connected to the chaotic nature of the Earth system that arises from complex interactions between the ocean, atmosphere, land, bio-

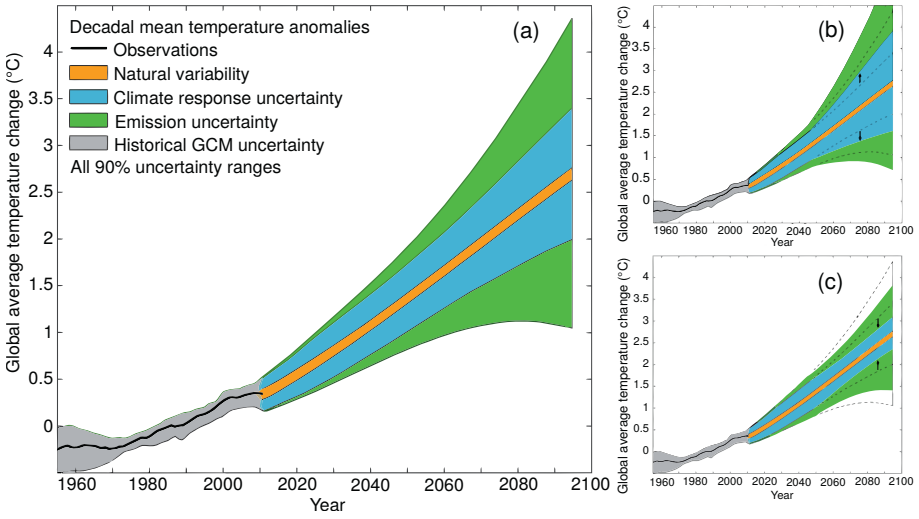

Figure 2.3.: Schematic illustrating the importance of different sources of uncertainties in climate model projections and their evolution in time. (a) Time series of the anomaly of the decadal and global mean surface temperature relative to the period 1961–1980. The black line shows the historical observations with estimates of uncertainty from climate models (gray). The remaining colors show different sources of uncertainty in future climate projections: Natural variability (orange), climate response uncertainty (blue) and emission uncertainty (green) (Hawkins & Sutton, 2009, 2010). Climate response uncertainty can (b) increase in newer generations of climate models when a new process is discovered to be relevant or (c) decrease with additional model improvements and observational constraints. Taken from Cubasch et al. (2013).

sphere and cryosphere (Cubasch et al., 2013). It constitutes a fundamental limit of how precisely we can project the future climate since it is inherent in the Earth system and cannot be eliminated by more knowledge and more advanced climate models. Natural variability is more relevant on regional and local scales than on continental or global scales. Further contributions to natural variability on longer time scales come from phenomena like the El Niño-Southern Oscillation (ENSO) or the North Atlantic Oscillation (NAO) and from externally (and thus explainable) events like volcanic eruptions and variations in the solar activity. Natural variability can be seen as the *noise* in the climate record as opposed to the anthropogenic *signal* (Cubasch et al., 2013). As illustrated by figure 2.3, the uncertainty associated with natural variability is constant over time.

The second source of uncertainty in climate model projections is *emission uncertainty*. This arises from the different possible trajectories in terms of future forcing (GHGs, aerosols, land use changes, etc.) humankind might take. Examples for these are the SSP-based experiments given by ScenarioMIP that include

a variety of different scenarios from a sustainable future to a full fossil fuel-based development (see section 2.1.2). A possible approach to quantify emission uncertainty is to assess the climate impact of these different trajectories. Since the emission uncertainty strongly depends on the future development of the human society, it cannot be reduced by improving climate models. In contrast to natural variability, the emission uncertainty increases over time in climate projections, since estimating forcings for the near future is easier than for the far future.

Finally, the third source of uncertainty in climate model projections is the *climate response uncertainty*, which comes from our imperfect knowledge of how the climate system will respond to future anthropogenic forcings. Due to the complexity of the Earth system, the future climate could develop in many different ways that are all consistent with our current knowledge and models (Cubasch et al., 2013). In the context of climate model ensembles, the climate response uncertainty is often also called *model uncertainty* and reflects the different responses of the different climate models to a given forcing. Even though all climate models are built on the same physical principles, they differ in terms of spatial resolution, processes included and parametrizations of unresolved processes. The latter can be thought of as different approximations that are necessary to represent processes that take place on scales smaller than the common size of grid boxes in modern global climate models (about $1° \times 1°$ horizontally), which is for example the case for some cloud processes and vegetation processes.

These differences in the climate models also give rise to different intensities of *climate feedbacks* (or even their presence/absence) in the models. A climate feedback is a mechanism that either amplifies (*positive feedback*) or diminishes (*negative feedback*) the effect of an external forcing. An example of a strong positive feedback is the water vapor feedback, in which the increased surface temperature (caused by anthropogenic forcing) leads to an enhanced evaporation of water which enhances the amount of water vapor in the atmosphere. Since water vapor itself is a powerful GHG, this amplifies the effect of the anthropogenic forcing by further increasing the surface temperatures (Cubasch et al., 2013). Further examples and a mathematical framework for the analysis of feedbacks are given in section 2.2.1.

As sciences evolves, representations of already included processes can be improved in climate models. Moreover, new geophysical and biogeochemical processes can be added to them. On the one hand, this can increase the climate response uncertainty when a new process is discovered to be relevant (Cubasch et al., 2013; see figure 2.3b). However, such an increase corresponds to a previ-

ously unmeasured uncertainty. An example for this has recently happened in CMIP6: most likely due to changes in the cloud representation of the models the spread in the projected global mean near-surface air temperature (GSAT) caused by a doubling of the atmospheric CO_2 concentration has substantially increased in CMIP6 compared to older CMIP generations (Zelinka et al., 2020). On the other hand, the climate response uncertainty can decrease with additional model improvements and better understanding of the Earth system (see figure 2.3c). Moreover, it can also be reduced by observational constraints, which is the main topic of this thesis.

2.2. Climate Sensitivity

Climate sensitivity refers to the change in the GSAT that results from a change in the radiative forcing. In other words, it describes how sensitive the climate system is to an external forcing. The source of this forcing might either be natural (changes in the solar activity, volcanic eruptions, etc.) or anthropogenic (emissions of GHGs, land use changes, etc.).

2.2.1. Climate Feedbacks

As already described in section 2.1.3, the effects of an external forcing acting on the climate system can additionally be amplified or diminished by climate feedbacks. Thus, feedback processes play a crucial role in the evaluation of climate sensitivity. Figure 2.4 shows an overview of important feedbacks in the Earth system with their corresponding time scales on which they operate.

An example for a positive feedback is the already mentioned *water vapor feedback*. Being the primary GHG in the Earth's atmosphere, water vapor is the largest contributor to the natural greenhouse effect. Since its amount in the atmosphere is mainly controlled by the air temperature and anthropogenic emissions of water vapor are negligible, the influence of water vapor on the climate system is described as a feedback mechanism and not as an external forcing (Myhre et al., 2013). Basis of this feedback is the enhanced evaporation of water with increasing air temperatures. Each degree of warming allows the atmosphere to retain about 7 % more water vapor (Myhre et al., 2013), which closes the positive feedback loop by further increasing air temperatures through the greenhouse effect. With a typical residence time of water vapor in the atmosphere of several days, the water vapor feedback operates on relatively short

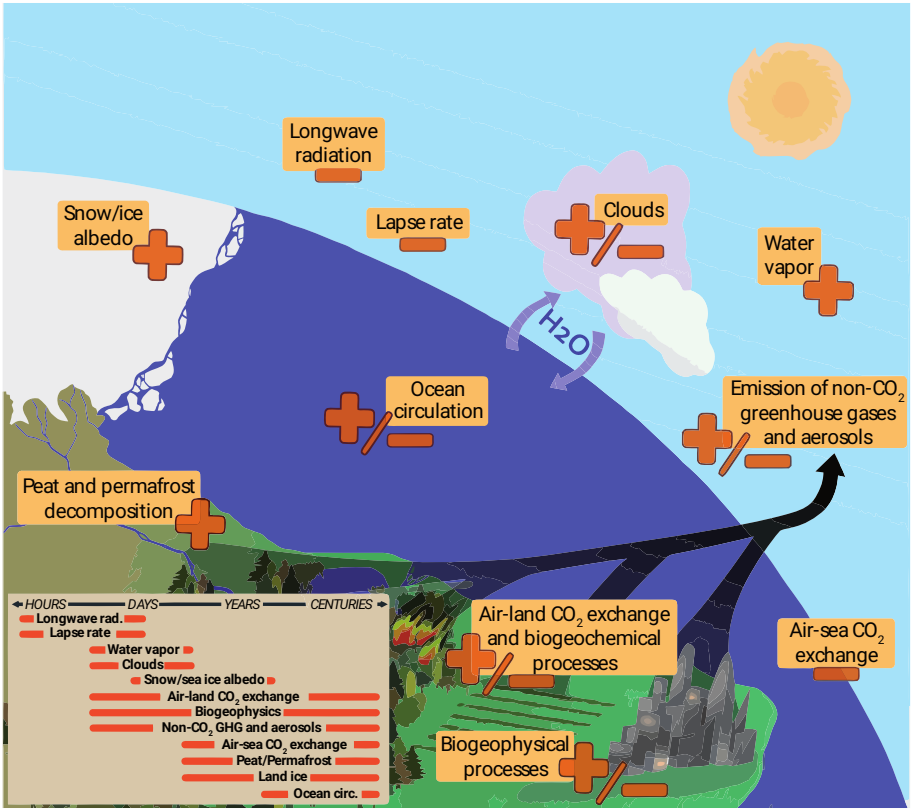

Figure 2.4.: Climate feedbacks and corresponding time scales. "+" refers to positive feedbacks, which amplify the effect of the external forcing (e.g. the water vapor feedback). "-" refers to negative feedbacks, which diminish the effect of the external forcing (e.g. the longwave radiation feedback). "+/-" refers to feedbacks which might be either positive or negative (e.g. the cloud feedback). The smaller box highlights the large differences in time scales for the various feedbacks. Taken from Cubasch et al. (2013).

time scales. As the largest positive feedback in the Earth system (Soden & Held, 2006), the water vapor feedback amplifies any initial forcing (e.g. caused by anthropogenic CO_2 emissions) by a typical factor between two and three, rendering water vapor a fundamental agent of climate change (Myhre et al., 2013). An example for a positive feedback that operates on longer time scales (several years) is the *snow/ice albedo feedback*, in which the surface albedo decreases as highly reflective ice and snow surfaces melt with global warming, exposing the darker and more absorbing surfaces below (Cubasch et al., 2013).

In contrast to positive feedbacks, negative feedbacks diminish the effect of an external forcing. An example for this is the *blackbody feedback* (also known as *Planck feedback* or *longwave radiation feedback*), which is the strongest negative feedback in the Earth system (Cubasch et al., 2013). It is based on the thermal electromagnetic radiation that any object with a non-zero temperature emits (the

so-called *blackbody radiation*). Since the power of this radiation strongly depends on the temperature of the object, higher surface temperatures of Earth increase the outgoing longwave radiation flux from the surface which reduces the effect of the external forcing and cools the planet.

For some domains of the Earth system, feedbacks can be positive and/or negative, since a variety of different mechanisms is involved. An example for this is the cloud feedback. Changes in clouds induced by climate change can cause both longwave (greenhouse warming) and shortwave (reflective cooling) effects, which both need to be considered for the overall cloud feedback (Boucher et al., 2013). Relevant cloud properties that may change as a response to an external forcing and that may alter the Earth's radiative budget are cloud cover, cloud optical thickness, cloud altitude and the geographical distribution of clouds. Examples for robust cloud feedback processes are the rise of high clouds in a warming climate which traps longwave radiation and enhances global warming and the reduction in mid- and low-level cloud cover which diminishes the reflection of incoming solar radiation and also increases the surface warming (Boucher et al., 2013). In global climate model ensembles, the overall cloud feedback shows a large range with positive and negative values, but tends to be slightly positive on average (Dufresne & Bony, 2008; Soden & Held, 2006; Vial et al., 2013; Zelinka et al., 2020). This large uncertainty in the cloud feedback is a major reason for uncertainties in the climate sensitivity of climate models (Boucher et al., 2013; Flato et al., 2013).

Further examples of feedbacks with positive and negative contributions are biogeochemical feedbacks. Negative contributions come from increased CO_2 fluxes into the land and ocean carbon reservoirs due to increased photosynthesis rates and CO_2 dissolution in the sea, respectively, which decrease the atmospheric CO_2 content and diminish global warming. An example for a positive contribution is the decreased solubility of CO_2 in water in a warmer climate, which reduces the atmosphere-ocean CO_2 flux and enhances climate change. More details on this are given in section 2.3.2.

2.2.2. Mathematical Framework for Feedbacks Analysis

The foundation for a basic mathematical framework for the analysis of climate feedbacks is a simple energy balance model (Gregory et al., 2009; Roe, 2009). Anthropogenic activities in the Earth system like the emissions of GHGs or aerosols introduce an external forcing to the climate system, which is quantified

with a radiative forcing F measured in Wm^{-2}. To restore a stable state, the climate system opposes this forcing with a climate response R, leading to a net energy flux of

$$N = F + R \tag{2.1}$$

into the system. Positive values of N, F and R indicate incoming fluxes; usually $F > 0$ and $R < 0$. On long time scales (multiple years), the net incoming radiative flux at the top of the atmosphere (TOA) and the net heat flux into the ocean are basically equal definitions of N since nearly all of the Earth's heat capacity resides in the ocean (Gregory et al., 2009). While $N \neq 0$, the climate system evolves; when $N = 0$ a new steady state has been reached.

To quantify the effects of different feedbacks, a reference system with a basic response needs to be defined, which is a crucial aspect of feedback analysis (Roe, 2009). Usually, the idealization of a blackbody Earth (without an atmosphere) is used for that: In equilibrium, the incoming solar irradiance is balanced with an outgoing thermal irradiance J_0 that solely depends on the global mean surface temperature T_0 following the Stefan–Boltzmann law

$$J_0 = -\sigma T_0^4. \tag{2.2}$$

$\sigma \approx 5.67\,\mathrm{Wm}^{-2}\mathrm{K}^{-4}$ is the Stefan–Boltzmann constant. To answer an external forcing F, the climate system reacts with a response R expressed by a change in the global mean surface temperature ΔT:

$$J_0 + R = -\sigma \left(T_0 + \Delta T\right)^4 \tag{2.3}$$

Since the temperature change caused by an anthropogenic forcing is much smaller than the equilibrium temperature $\Delta T \ll T_0 \approx 255\,\mathrm{K}$, a simple 1^{st}-order Taylor expansion can be used to linearize the blackbody response:

$$-\sigma \left(T_0 + \Delta T\right)^4 \approx J_0 - 4\sigma T_0^3 \cdot \Delta T \tag{2.4}$$

Thus, by comparing equations (2.3) and (2.4) the climate response R can be expressed as

$$R = -4\sigma T_0^3 \cdot \Delta T \coloneqq \lambda_{\mathrm{BB}} \cdot \Delta T \tag{2.5}$$

with the blackbody feedback parameter $\lambda_{\mathrm{BB}} \approx -3.8\,\mathrm{Wm}^{-2}\mathrm{K}^{-1}$. Results from climate models and analyses of observations confirm this linear relationship between R and ΔT (Gregory et al., 2004). However, the value of this linear

constant λ, the *climate feedback parameter*, is found to be considerably larger than the blackbody response ($\lambda \approx -1.0\,\mathrm{Wm^{-2}K^{-1}}$), indicating that additional processes affect the Earth's radiative balance: the climate feedbacks (Flato et al., 2013; Gregory et al., 2009). Since climate models suggest that the radiative effects of these additional feedbacks are also proportional to ΔT (Gregory & Webb, 2008), equation (2.5) can be adapted to

$$R = \lambda \cdot \Delta T = (\lambda_{\mathrm{BB}} + \lambda_{\mathrm{WV}} + \lambda_{\mathrm{Albedo}} + \lambda_{\mathrm{Cloud}} + \ldots) \cdot \Delta T. \tag{2.6}$$

λ_{WV} refers to the water vapor feedback, $\lambda_{\mathrm{Albedo}}$ to the snow/ice albedo feedback and λ_{Cloud} to the cloud feedback. Thus, the overall climate feedback parameter λ can be written as the sum of the individual feedback parameters λ_i:

$$\lambda = \sum_i \lambda_i \tag{2.7}$$

Positive values of λ_i indicate positive feedbacks (e.g. the water vapor feedback) and negative values indicate negative feedbacks (e.g. the blackbody feedback). This equation assumes that the individual radiative responses from the different feedbacks are independent, which is a reasonable first-order approximation but not entirely true (Soden et al., 2008).

2.2.3. Equilibrium and Effective Climate Sensitivity

- Physical Feedbacks (ECS)
  - ocean heat uptake (TCR)
  - different between effective climate sensitivity and equilibrium version
  - equations for ECS and TCR

2.3. The Global Carbon Cycle

Since one study presented in this thesis aims to reduce uncertainties in carbon cycle-related processes (Schlund, Eyring, et al., 2020; see chapter 6), this chapter introduces the scientific background of the global carbon cycle.

2.3.1. Overview

A schematic overview of the global carbon cycle is shown in figure 2.5. To quantify the carbon cycle, common units are parts per million (ppm) for the

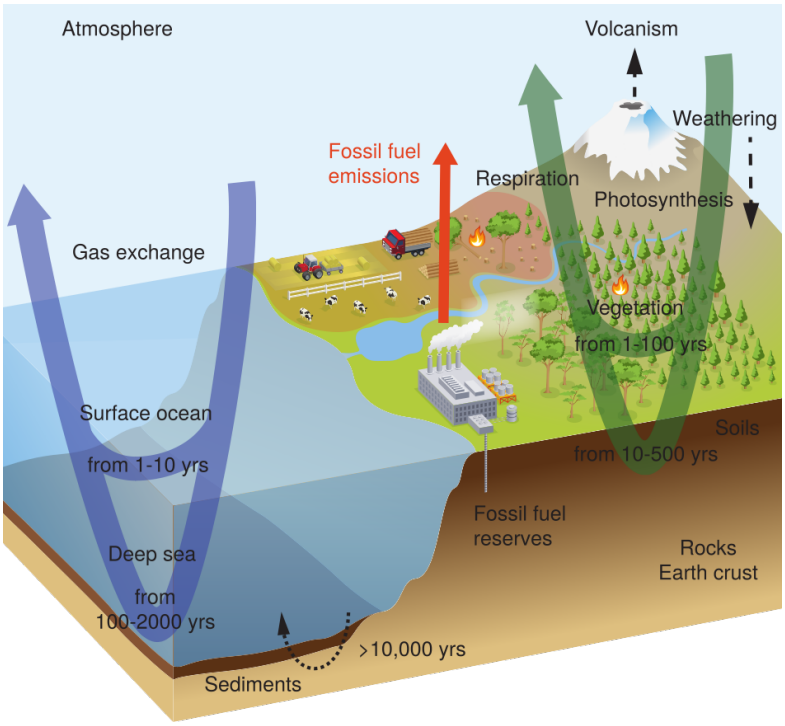

Figure 2.5.: Simplified schematic of the global carbon cycle including the typical turnover time scales for carbon transfers through the major reservoirs (atmosphere, land surface and ocean). Taken from Ciais et al. (2013).

atmospheric trace gas concentrations (dry-air mole fraction) and gigatonnes of carbon (GtC) or GtC yr^{-1} for the reservoirs masses or exchange fluxes, respectively. The carbon exchange processes between the different carbon reservoirs run on a wide range of time scales. Conceptually, one can distinguish between two domains of the global carbon cycle: a slow and a fast domain. The slow domain with turnover times (reservoir mass of carbon divided by exchange flux) of more than 10000 years consists of the large carbon stores in rocks and sediments which are connected to the rapid domain of the carbon cycle through volcanic emissions of CO_2, chemical weathering, erosion and sediment formation on the sea floor. These natural exchange fluxes between the slow and the fast domain are comparatively small (< 0.3 GtC yr^{-1}) and can be assumed as approximately constant in time over the last few centuries (Ciais et al., 2013).

The fast domain of the global carbon cycle consists of three main carbon reservoirs: the atmosphere, the terrestrial biosphere and the ocean. In the atmosphere, carbon is mainly stored in trace gases, with CO_2 as the major component with a current (2019) concentration of about 410 ppm (Friedlingstein et al., 2019). Additional contributors to the atmospheric carbon content are the trace gas methane (CH_4), the trace gas carbon monoxide (CO), hydrocarbons, black

carbon aerosols and organic compounds (Ciais et al., 2013). Carbon in the terrestrial biosphere is mainly stored as organic compounds, with about 450–650 GtC in the living vegetation biomass, 1500–2400 GtC in dead organic matter in litter and soils and about 1700 GtC in permafrost soils (Ciais et al., 2013). The main component of the oceanic carbon reservoir is dissolved inorganic carbon (carbonic acid, bicarbonate ions and carbonate ions) with about 38000 GtC. Further carbon is stored as dissolved organic carbon (about 700 GtC), in surface sediments (about 1750 GtC) and in marine biota (about 3 GtC, predominantly phytoplankton and other microorganisms) (Ciais et al., 2013; Friedlingstein et al., 2019).

In the fast domain of the global carbon cycle, reservoir turnover times range from seconds to millennia. In contrast to the slow domain, the carbon exchange fluxes within the fast domain of the carbon cycle are much higher. One major group of exchange processes in the fast domain connects the atmosphere and the terrestrial biosphere. CO_2 is removed from the atmosphere by plant photosynthesis with about 120 GtC yr^{-1} (Ciais et al., 2013). This process is also known as Gross Primary Productivity (GPP). The carbon fixed into plants can be released back into the atmosphere by autotrophic (plant) and heterotrophic (soil microbial and animal) respiration and additional disturbance processes like fires (Ciais et al., 2013). Since the land CO_2 uptake by photosynthesis occurs only during the growing season, whereas respiration occurs nearly all year, the larger amount of vegetation in the Northern hemisphere (due to the larger land mass) gives rise to a seasonal cycle of the atmospheric CO_2 concentration (Keeling et al., 1995). This seasonal cycle reflects the phase of the global carbon cycle and shows a maximum of the atmospheric CO_2 concentration in the Northern hemisphere winter (net CO_2 flux into atmosphere due to respiration) and a minimum during the Northern hemisphere summer (net CO_2 flux into the land due to photosynthesis). Another major carbon exchange process connects the atmosphere and the ocean. Atmospheric CO_2 is exchanged with the surface ocean through gas exchange, which is driven by the partial CO_2 pressure difference between the air and the sea (Ciais et al., 2013).

2.3.2. Anthropogenic Perturbations

Before the Industrial Era, the global carbon cycle was roughly in a dynamic equilibrium, which means that exchange fluxes balanced each other and the amount of carbon in the different reservoirs did neither increase nor decrease. This

can be inferred from ice core measurements, which show an almost constant atmospheric CO_2 concentration over the last several thousand years before the Industrial Revolution in the 19th century (Ciais et al., 2013). Since the beginning of the Industrial Era, humanity is constantly emitting carbon-based GHGs (e.g. CO_2 and CH_4) into the atmosphere. Especially the atmospheric CO_2 concentration has substantially increased, which has already been shown by Charles D. Keeling in 1976 by his continuous CO_2 measurements at Mauna Loa, Hawaii that started in 1958 (Keeling et al., 1976; see figure 2.6). From 1958, the atmospheric CO_2 concentration at Mauna Loa has steadily increased by about 100 ppm to 410 ppm in the year 2019 (Keeling et al., 2005). In addition to the steady increase, the so-called *Keeling Curve* is further superimposed with the seasonal CO_2 cycle, which gives rise to local maxima of the atmospheric CO_2 concentration in the Northern hemisphere winter and local minima in the Northern hemisphere summer (Keeling et al., 1995; see section 2.3.1). Due to its location in the middle of the Pacific Ocean, the Mauna Loa Observatory offers perfect conditions for CO_2 measurements by being far away from big population centers. Moreover, its elevation of more than 3000 m provides access to the well-mixed air of the Pacific Ocean in high altitudes, which prevents any interference from the vegetation present on the Hawaiian Islands.

Apart from warming the Earth by altering its radiation budget, the anthropogenically emitted CO_2 directly influences the carbon exchange fluxes of the global carbon cycle. Due to the excessive carbon in the atmosphere, there is now a net carbon flux from the atmosphere into the land and ocean reservoirs (see figure 2.7). Thus, the carbon cycle is not in a steady state anymore. In the decade 2009–2018, anthropogenic activities caused net carbon fluxes of 3.2 GtC yr^{-1} from the atmosphere into the terrestrial biosphere due to increased plant photosynthesis and 2.5 GtC yr^{-1} from the atmosphere into the ocean due to increase dissolution of CO_2 into the sea (Friedlingstein et al., 2019). In the same time, the amount of carbon in the atmosphere reservoir increased with a rate of 4.9 GtC yr^{-1}, indicating that only about half of the anthropogenic CO_2 emissions in the last decade remained in the atmosphere (Friedlingstein et al., 2019) where they can act as GHG.

Thus, this removal of CO_2 from the atmosphere actively slows down global warming. However, whether this benefit will persist in the future remains unclear, which is primarily linked to two feedback processes connecting the physical climate system and the global carbon cycle: the *concentration-carbon feedback* and the *climate-carbon feedback* (M. Collins et al., 2013; Friedlingstein et

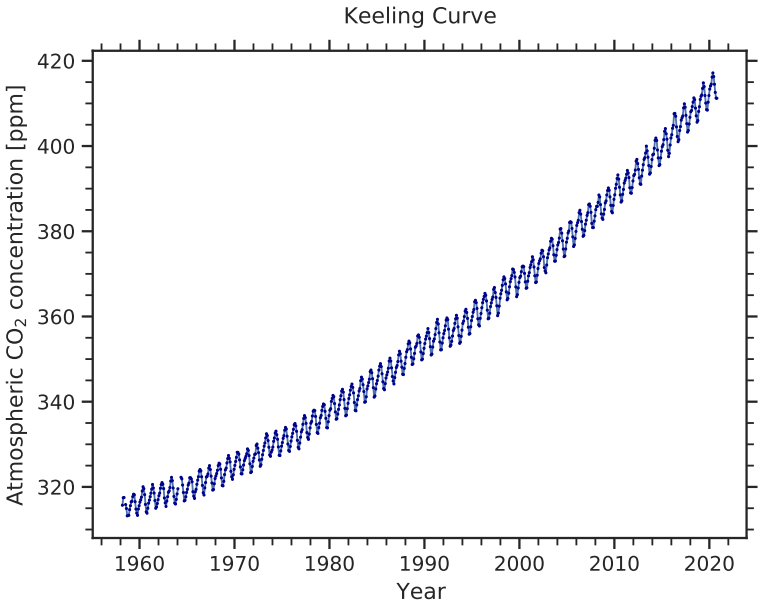

Figure 2.6.: The Keeling Curve: monthly-mean atmospheric CO_2 concentration at the Mauna Loa Observatory, Hawaii (19.5 °N, 155.6 °W; elevation: 3397 m) from 1958 to 2019 (Keeling et al., 2005). The steady increase of the atmospheric CO_2 concentration is superimposed with a seasonal oscillation caused by the seasonal CO_2 cycle (see section 2.3.1).

al., 2006; Gregory et al., 2009). For the terrestrial biosphere, the concentration-carbon feedback is connected to the *CO_2 fertilization effect* (Walker et al., 2020), that causes an increase of photosynthesis rates when the atmospheric CO_2 concentration increases, which in turns removes CO_2 from the atmosphere, forming a negative feedback. For the ocean, the concentration-carbon feedback is negative as well. In this case, an elevated atmospheric CO_2 concentration causes an increased dissolution of CO_2 into the sea, which increases the ocean carbon uptake. On the other hand, the climate-carbon feedback is thought to be positive for both the terrestrial biosphere and the ocean (Gregory et al., 2009). In the first case, temperature and precipitation changes due to anthropogenic activities decrease the land carbon uptake because of increased temperature and water stress on photosynthesis and higher ecosystem respiration costs, which accelerates global warming due to more CO_2 that remains in the atmosphere. For the ocean, increased temperatures lead to a reduction of vertical transport in the ocean resulting from increased stability and reduced solubility of CO_2 in the sea, which reduces the ocean carbon uptake and enhances climate change (Gregory et al., 2009).

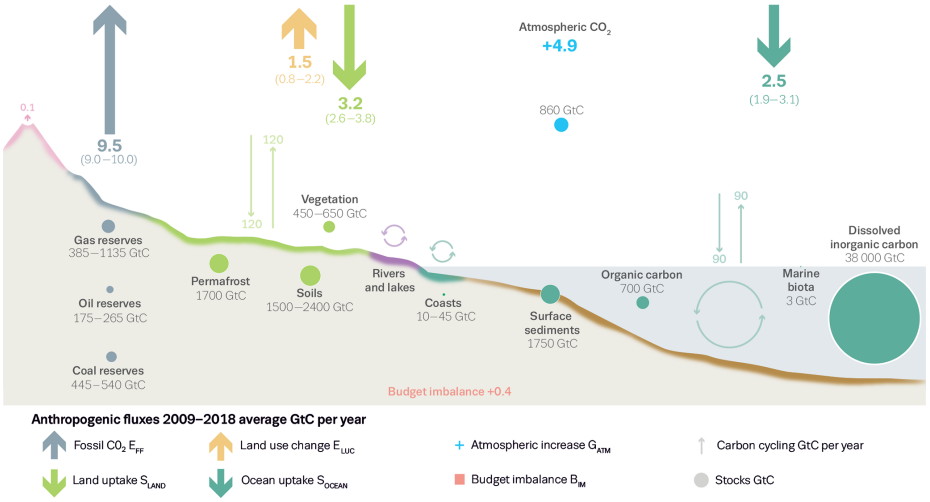

Figure 2.7.: Schematic representation of the overall perturbation of the global carbon cycle caused by anthropogenic activities, averaged globally for the decade 2009–2018. Arrows represent carbon exchange fluxes; circles carbon reservoirs. More details are given in the legend of this figure. Taken from Friedlingstein et al. (2019).

2.4. Techniques to Reduce Uncertainties in Climate Model Projections

- Problems with multi-model analysis (search for refs in Schlund et al., ESD, 2020) -> models are not independent, multi-model ensemble is not "real" statistical sample

- Process-based weighting (Knutti + MDER)
- emergent constraints
- Wenzel et al., Nature (2016) as example (refer to carbon cycle chapter)
- Review of ECS emergent constraints is given in chapter on Schlund et al., ESD (2020)

3. Improving Routine Climate Model Evaluation

TBA.

4. Assessment of Policy-Relevant Climate Metrics in CMIP6

TBA.

5. Evaluation of Emergent Constraints on the Effective Climate Sensitivity in CMIP6

TBA.

6. Constraining Uncertainties in Future Gross Primary Productivity with Machine Learning

TBA.

7. Summary and Outlook

TBA.

Appendix

A. TBA

A.1. test

test

hi The Effective Climate Sensitivity (ECS) is really cool. I like it very much!

This is e.g. without an "at" and this is it with an "at" e.g. difference? Test space. Real dot!

E.g.blaa. E.g. blaaaa. i.e.blaaaa, i.e. blaa.

These are really cool papers: (Schlund, Lauer, et al., 2020; Schlund, Eyring, et al., 2020)

autocite: (Lauer et al., 2018)

cite: Lauer et al., 2010 (Anav et al., 2015) (Anav et al., 2013) (Allen & Ingram, 2002)

textcite: Lauer et al. (2010)

And this one, too: (Lauer et al., 2020)

This is a reference to the equation: equation (1)

Three authors: (Bao et al., 2020)

Many many authors: (Eyring et al., 2020)

```
input <iostream>
```

$$c_{k_1,k_2} := 1200 \log_2 \left(\frac{f_1^{(k_2)}}{f_1^{(k_1)}} \right) \text{ cents.} \tag{1}$$

B. TBA

TBA.

Table 1.: The effects of treatments X and Y on the four groups studied.

Groups	**Treatment X**	**Treatment Y**
1	0.2	0.8
2	0.17	0.7
3	0.24	0.75
4	0.68	0.3

Semitones	Interval	c / cents (ET)	c / cents (JI)
0	Perfect unison	0	0
1	Minor second	100	112
2	Major second	200	204
3	Minor third	300	316
4	Major third	400	386
5	Perfect fourth	500	498
6	Augmented fourth	600	590
7	Perfect fifth	700	702
8	Minor sixth	800	814
9	Major sixth	900	884
10	Minor seventh	1000	996
11	Major seventh	1100	1088
12	Perfect octave	1200	1200

Table 2.: Logarithmic frequency ratios c of certain intervals in the equal temperament (ET) and the just intonation (JI). x cents correspond to a frequency ratio of $2^{x/1200}$.

List of Acronyms

Integrated Author's References

Bock, L., Lauer, A., **Schlund**, **M.**, Barreiro, M., Bellouin, N., Jones, C., Meehl, G. A., Predoi, V., Roberts, M. J., & Eyring, V. (2020). Quantifying Progress Across Different CMIP Phases With the ESMValTool. *Journal of Geophysical Research: Atmospheres*, *125*(21). https://doi.org/10.1029/2019jd032321

Eyring, V., Bock, L., Lauer, A., Righi, M., **Schlund**, **M.**, Andela, B., Arnone, E., Bellprat, O., Brötz, B., Caron, L.-P., Carvalhais, N., Cionni, I., Cortesi, N., Crezee, B., Davin, E. L., Davini, P., Debeire, K., de Mora, L., Deser, C., Docquier, D., Earnshaw, P., Ehbrecht, C., Gier, B. K., Gonzalez-Reviriego, N., Goodman, P., Hagemann, S., Hardiman, S., Hassler, B., Hunter, A., Kadow, C., Kindermann, S., Koirala, S., Koldunov, N., Lejeune, Q., Lembo, V., Lovato, T., Lucarini, V., Massonnet, F., Müller, B., Pandde, A., Pérez-Zanón, N., Phillips, A., Predoi, V., Russell, J., Sellar, A., Serva, F., Stacke, T., Swaminathan, R., Torralba, V., Vegas-Regidor, J., von Hardenberg, J., Weigel, K., & Zimmermann, K. (2020). Earth System Model Evaluation Tool (ESMValTool) v2.0 – an extended set of large-scale diagnostics for quasi-operational and comprehensive evaluation of Earth system models in CMIP. *Geoscientific Model Development*, *13*(7), 3383–3438. https://doi.org/10.5194/gmd-13-3383-2020

Lauer, A., Eyring, V., Bellprat, O., Bock, L., Gier, B. K., Hunter, A., Lorenz, R., Pérez-Zanón, N., Righi, M., **Schlund**, **M.**, Senftleben, D., Weigel, K., & Zechlau, S. (2020). Earth System Model Evaluation Tool (ESMValTool) v2.0 – diagnostics for emergent constraints and future projections from Earth system models in CMIP. *Geoscientific Model Development*, *13*(9), 4205–4228. https://doi.org/10.5194/gmd-13-4205-2020

Meehl, G. A., Senior, C. A., Eyring, V., Flato, G., Lamarque, J.-F., Stouffer, R. J., Taylor, K. E., & **Schlund**, **M.** (2020). Context for interpreting equilibrium climate sensitivity and transient climate response from the CMIP6 Earth system models. *Science Advances*, *6*(26), eaba1981. https://doi.org/10.1126/sciadv.aba1981

Righi, M., Andela, B., Eyring, V., Lauer, A., Predoi, V., **Schlund**, **M.**, Vegas-Regidor, J., Bock, L., Brotz, B., de Mora, L., Diblen, F., Dreyer, L., Drost, N., Earnshaw, P., Hassler, B., Koldunov, N., Little, B., Tomas, S. L., & Zimmermann, K. (2020). Earth System Model Evaluation Tool (ESMValTool) v2.0-technical overview. *Geoscientific Model Development*, *13*(3), 1179–1199. https://doi.org/10.5194/gmd-13-1179-2020

Schlund, **M.**, Lauer, A., Gentine, P., Sherwood, S. C., & Eyring, V. (2020). Emergent constraints on Equilibrium Climate Sensitivity in CMIP5: do they hold for CMIP6? *Earth System Dynamics Discussions*, *2020*, 1–40. https://doi.org/10.5194/esd-2020-49

Schlund, **M.**, Eyring, V., Camps-Valls, G., Friedlingstein, P., Gentine, P., & Reichstein, M. (2020). Constraining Uncertainty in Projected Gross Primary Production With Machine Learning. *Journal of Geophysical Research: Biogeosciences*, *125*(11), e2019JG005619. https://doi.org/10.1029/2019jg005619

Weigel, K., Bock, L., Gier, B. K., Lauer, A., Righi, M., **Schlund**, **M.**, Adeniyi, K., Andela, B., Arnone, E., Berg, P., Caron, L.-P., Cionni, I., Corti, S., Drost, N., Hunter, A., Lledó, L., Mohr, C. W., Paçal, A., Pérez-Zanón, N., Predoi, V., Sandstad, M., Sillmann, J., Sterl, A., Vegas-Regidor, J., von Hardenberg, J., & Eyring, V. (2020). Earth System Model Evaluation Tool (ESMValTool) v2.0 – diagnostics for extreme events, regional and impact evaluation and analysis of Earth system models in CMIP. *Geoscientific Model Development Discussions*, *in review*, 1–43. https://doi.org/10.5194/gmd-2020-244

References

Allen, M. R., & Ingram, W. J. (2002). Constraints on future changes in climate and the hydrologic cycle. *Nature*, *419*(6903), 224–+. https://doi.org/10.1038/nature01092

Anav, A., Friedlingstein, P., Kidston, M., Bopp, L., Ciais, P., Cox, P., Jones, C., Jung, M., Myneni, R., & Zhu, Z. (2013). Evaluating the Land and Ocean Components of the Global Carbon Cycle in the CMIP5 Earth System Models. *Journal of Climate*, *26*(18), 6801–6843. https://doi.org/10.1175/Jcli-D-12-00417.1

Anav, A., Friedlingstein, P., Beer, C., Ciais, P., Harper, A., Jones, C., Murray-Tortarolo, G., Papale, D., Parazoo, N. C., Peylin, P., Piao, S., Sitch, S., Viovy, N., Wiltshire, A., & Zhao, M. (2015). Spatiotemporal patterns of terrestrial gross primary production: A review. *Reviews of Geophysics*, *53*(3), 785–818. https://doi.org/10.1002/2015rg000483

Bao, Y., Song, Z. Y., & Qiao, F. L. (2020). FIO-ESM Version 2.0: Model Description and Evaluation. *Journal of Geophysical Research-Oceans*, *125*(6). https://doi.org/10.1029/2019JC016036

Bock, L., Lauer, A., **Schlund**, **M.**, Barreiro, M., Bellouin, N., Jones, C., Meehl, G. A., Predoi, V., Roberts, M. J., & Eyring, V. (2020). Quantifying Progress Across Different CMIP Phases With the ESMValTool. *Journal of Geophysical Research: Atmospheres*, *125*(21). https://doi.org/10.1029/2019jd032321

Boucher, O., Randall, D., Artaxo, P., Bretherton, C., Feingold, G., Forster, P., Kerminen, V.-M., Kondo, Y., Liao, H., & Lohmann, U. (2013). Clouds and Aerosols. Cambridge University Press. https://www.ipcc.ch/site/assets/uploads/2018/02/WG1AR5_Chapter07_FINAL-1.pdf

Ciais, P., Sabine, C., Bala, G., Bopp, L., Brovkin, V., Canadell, J., Chhabra, A., DeFries, R., Galloway, J., & Heimann, M. (2013). Carbon and Other Biogeochemical Cycles. Cambridge University Press. https://www.ipcc.ch/site/assets/uploads/2018/02/WG1AR5_Chapter06_FINAL.pdf

Collins, M., Knutti, R., Arblaster, J., Dufresne, J.-L., Fichefet, T., Friedlingstein, P., Gao, X., Gutowski, W. J., Johns, T., & Krinner, G. (2013). Long-term Cli-

mate Change: Projections, Commitments and Irreversibility. Cambridge University Press. https://www.ipcc.ch/site/assets/uploads/2018/02/WG1AR5_Chapter12_FINAL.pdf

Collins, W. J., Lamarque, J.-F., Schulz, M., Boucher, O., Eyring, V., Hegglin, M. I., Maycock, A., Myhre, G., Prather, M., Shindell, D., & Smith, S. J. (2017). AerChemMIP: quantifying the effects of chemistry and aerosols in CMIP6. *Geoscientific Model Development*, *10*(2), 585–607. https://doi.org/10.5194/gmd-10-585-2017

Cubasch, U., Wuebbles, D., Chen, D., Facchini, M. C., Frame, D., Mahowald, N., & Winther, J.-G. (2013). Introduction. Cambridge University Press. https://www.ipcc.ch/site/assets/uploads/2017/09/WG1AR5_Chapter01_FINAL.pdf

Dufresne, J.-L., & Bony, S. (2008). An Assessment of the Primary Sources of Spread of Global Warming Estimates from Coupled Atmosphere–Ocean Models. *Journal of Climate*, *21*(19), 5135–5144. https://doi.org/10.1175/2008jcli2239.1

Eyring, V., Bony, S., Meehl, G. A., Senior, C. A., Stevens, B., Stouffer, R. J., & Taylor, K. E. (2016). Overview of the Coupled Model Intercomparison Project Phase 6 (CMIP6) experimental design and organization. *Geoscientific Model Development*, *9*(5), 1937–1958. https://doi.org/10.5194/gmd-9-1937-2016

Eyring, V., Bock, L., Lauer, A., Righi, M., **Schlund**, **M.**, Andela, B., Arnone, E., Bellprat, O., Brötz, B., Caron, L.-P., Carvalhais, N., Cionni, I., Cortesi, N., Crezee, B., Davin, E. L., Davini, P., Debeire, K., de Mora, L., Deser, C., Docquier, D., Earnshaw, P., Ehbrecht, C., Gier, B. K., Gonzalez-Reviriego, N., Goodman, P., Hagemann, S., Hardiman, S., Hassler, B., Hunter, A., Kadow, C., Kindermann, S., Koirala, S., Koldunov, N., Lejeune, Q., Lembo, V., Lovato, T., Lucarini, V., Massonnet, F., Müller, B., Pandde, A., Pérez-Zanón, N., Phillips, A., Predoi, V., Russell, J., Sellar, A., Serva, F., Stacke, T., Swaminathan, R., Torralba, V., Vegas-Regidor, J., von Hardenberg, J., Weigel, K., & Zimmermann, K. (2020). Earth System Model Evaluation Tool (ESMValTool) v2.0 – an extended set of large-scale diagnostics for quasi-operational and comprehensive evaluation of Earth system models in CMIP. *Geoscientific Model Development*, *13*(7), 3383–3438. https://doi.org/10.5194/gmd-13-3383-2020

Flato, G. M. (2011). Earth system models: an overview. *Wiley Interdisciplinary Reviews: Climate Change*, *2*(6), 783–800. https://doi.org/10.1002/wcc.148

Flato, G. M., Marotzke, J., Abiodun, B., Braconnot, P., Chou, S. C., Collins, W., Cox, P., Driouech, F., Emori, S., Eyring, V., Forest, C., Gleckler, P., Guilyardi, E., Jakob, C., Kattsov, V., Reason, C., & Rummukainen, M. (2013). Evaluation of Climate Models. Cambridge University Press. https://www.ipcc.ch/site/assets/uploads/2018/02/WG1AR5_Chapter09_FINAL.pdf

Friedlingstein, P., Cox, P., Betts, R., Bopp, L., Von Bloh, W., Brovkin, V., Cadule, P., Doney, S., Eby, M., Fung, I., Bala, G., John, J., Jones, C., Joos, F., Kato, T., Kawamiya, M., Knorr, W., Lindsay, K., Matthews, H. D., Raddatz, T., Rayner, P., Reick, C., Roeckner, E., Schnitzler, K. G., Schnur, R., Strassmann, K., Weaver, A. J., Yoshikawa, C., & Zeng, N. (2006). Climate-carbon cycle feedback analysis: Results from the (CMIP)-M-4 model intercomparison. *Journal of Climate*, *19*(14), 3337–3353. https://doi.org/10.1175/Jcli3800.1

Friedlingstein, P., Jones, M. W., O'Sullivan, M., Andrew, R. M., Hauck, J., Peters, G. P., Peters, W., Pongratz, J., Sitch, S., Le Quere, C., Bakker, D. C. E., Canadell, J. G., Ciais, P., Jackson, R. B., Anthoni, P., Barbero, L., Bastos, A., Bastrikov, V., Becker, M., Bopp, L., Buitenhuis, E., Chandra, N., Chevallier, F., Chini, L. P., Currie, K. I., Feely, R. A., Gehlen, M., Gilfillan, D., Gkritzalis, T., Goll, D. S., Gruber, N., Gutekunst, S., Harris, I., Haverd, V., Houghton, R. A., Hurtt, G., Ilyina, T., Jain, A. K., Joetzjer, E., Kaplan, J. O., Kato, E., Goldewijk, K. K., Korsbakken, J. I., Landschutzer, P., Lauvset, S. K., Lefevre, N., Lenton, A., Lienert, S., Lombardozzi, D., Marland, G., McGuire, P. C., Melton, J. R., Metzl, N., Munro, D. R., Nabel, J. E. M. S., Nakaoka, S. I., Neill, C., Omar, A. M., Ono, T., Peregon, A., Pierrot, D., Poulter, B., Rehder, G., Resplandy, L., Robertson, E., Rodenbeck, C., Seferian, R., Schwinger, J., Smith, N., Tans, P. P., Tian, H. Q., Tilbrook, B., Tubiello, F. N., van der Werf, G. R., Wiltshire, A. J., & Zaehle, S. (2019). Global Carbon Budget 2019. *Earth System Science Data*, *11*(4), 1783–1838. https://doi.org/10.5194/essd-11-1783-2019

Gregory, J. M., Ingram, W. J., Palmer, M. A., Jones, G. S., Stott, P. A., Thorpe, R. B., Lowe, J. A., Johns, T. C., & Williams, K. D. (2004). A new method for diagnosing radiative forcing and climate sensitivity. *Geophysical Research Letters*, *31*(3). https://doi.org/10.1029/2003gl018747

Gregory, J. M., Jones, C. D., Cadule, P., & Friedlingstein, P. (2009). Quantifying Carbon Cycle Feedbacks. *Journal of Climate*, *22*(19), 5232–5250. https://doi.org/10.1175/2009jcli2949.1

Gregory, J. M., & Webb, M. (2008). Tropospheric Adjustment Induces a Cloud Component in CO2 Forcing. *Journal of Climate*, *21*(1), 58–71. https://doi.org/10.1175/2007jcli1834.1

Hawkins, E., & Sutton, R. (2009). The Potential to Narrow Uncertainty in Regional Climate Predictions. *Bulletin of the American Meteorological Society*, *90*(8), 1095–1108. https://doi.org/10.1175/2009bams2607.1

Hawkins, E., & Sutton, R. (2010). The potential to narrow uncertainty in projections of regional precipitation change. *Climate Dynamics*, *37*(1-2), 407–418. https://doi.org/10.1007/s00382-010-0810-6

Jones, C. D., Arora, V., Friedlingstein, P., Bopp, L., Brovkin, V., Dunne, J., Graven, H., Hoffman, F., Ilyina, T., John, J. G., Jung, M., Kawamiya, M., Koven, C., Pongratz, J., Raddatz, T., Randerson, J. T., & Zaehle, S. (2016). C4MIP – The Coupled Climate–Carbon Cycle Model Intercomparison Project: experimental protocol for CMIP6. *Geoscientific Model Development*, *9*(8), 2853–2880. https://doi.org/10.5194/gmd-9-2853-2016

Keeling, C. D., Piper, S. C., Bacastow, R. B., Wahlen, M., Whorf, T. P., Heimann, M., & Meijer, H. A. (2005). Atmospheric CO2 and 13CO2 exchange with the terrestrial biosphere and oceans from 1978 to 2000: Observations and carbon cycle implications.

Keeling, C. D., Whorf, T. P., Wahlen, M., & Vanderplicht, J. (1995). Interannual Extremes in the Rate of Rise of Atmospheric Carbon-Dioxide since 1980. *Nature*, *375*(6533), 666–670. https://doi.org/10.1038/375666a0

Keeling, C. D., Bacastow, R. B., Bainbridge, A. E., Jr., C. A. E., Guenther, P. R., Waterman, L. S., & Chin, J. F. S. (1976). Atmospheric carbon dioxide variations at Mauna Loa Observatory, Hawaii. *Tellus*, *28*(6), 538–551. https://doi.org/10.3402/tellusa.v28i6.11322

Lauer, A., Hamilton, K., Wang, Y. Q., Phillips, V. T. J., & Bennartz, R. (2010). The Impact of Global Warming on Marine Boundary Layer Clouds over the Eastern Pacific-A Regional Model Study. *Journal of Climate*, *23*(21), 5844–5863. https://doi.org/10.1175/2010jcli3666.1

Lauer, A., Jones, C., Eyring, V., Evaldsson, M., Stefan, H. A., Makela, J., Martin, G., Roehrig, R., & Wang, S. Y. (2018). Process-level improvements in CMIP5 models and their impact on tropical variability, the Southern Ocean, and monsoons. *Earth System Dynamics*, *9*(1), 33–67. https://doi.org/10.5194/esd-9-33-2018

Lauer, A., Eyring, V., Bellprat, O., Bock, L., Gier, B. K., Hunter, A., Lorenz, R., Pérez-Zanón, N., Righi, M., **Schlund**, **M.**, Senftleben, D., Weigel, K., &

Zechlau, S. (2020). Earth System Model Evaluation Tool (ESMValTool) v2.0 – diagnostics for emergent constraints and future projections from Earth system models in CMIP. *Geoscientific Model Development*, *13*(9), 4205–4228. https://doi.org/10.5194/gmd-13-4205-2020

Meehl, G. A., Senior, C. A., Eyring, V., Flato, G., Lamarque, J.-F., Stouffer, R. J., Taylor, K. E., & **Schlund**, **M.** (2020). Context for interpreting equilibrium climate sensitivity and transient climate response from the CMIP6 Earth system models. *Science Advances*, *6*(26), eaba1981. https://doi.org/10.1126/sciadv.aba1981

Myhre, G., Shindell, D., Bréon, F.-M., Collins, W., Fuglestvedt, J., Huang, J., Koch, D., Lamarque, J.-F., Lee, D., Mendoza, B., Nakajima, T., Robock, A., Stephens, G., Takemura, T., & Zhang, H. (2013). Anthropogenic and Natural Radiative Forcing. Cambridge University Press. https://www.ipcc.ch/site/assets/uploads/2018/02/WG1AR5_Chapter08_FINAL.pdf

O'Neill, B. C., Kriegler, E., Ebi, K. L., Kemp-Benedict, E., Riahi, K., Rothman, D. S., van Ruijven, B. J., van Vuuren, D. P., Birkmann, J., Kok, K., Levy, M., & Solecki, W. (2017). The roads ahead: Narratives for shared socioeconomic pathways describing world futures in the 21st century. *Global Environmental Change*, *42*, 169–180. https://doi.org/10.1016/j.gloenvcha.2015.01.004

O'Neill, B. C., Kriegler, E., Riahi, K., Ebi, K. L., Hallegatte, S., Carter, T. R., Mathur, R., & van Vuuren, D. P. (2013). A new scenario framework for climate change research: the concept of shared socioeconomic pathways. *Climatic Change*, *122*(3), 387–400. https://doi.org/10.1007/s10584-013-0905-2

O'Neill, B. C., Tebaldi, C., van Vuuren, D. P., Eyring, V., Friedlingstein, P., Hurtt, G., Knutti, R., Kriegler, E., Lamarque, J.-F., Lowe, J., Meehl, G. A., Moss, R., Riahi, K., & Sanderson, B. M. (2016). The Scenario Model Intercomparison Project (ScenarioMIP) for CMIP6. *Geoscientific Model Development*, *9*(9), 3461–3482. https://doi.org/10.5194/gmd-9-3461-2016

Riahi, K., van Vuuren, D. P., Kriegler, E., Edmonds, J., O'Neill, B. C., Fujimori, S., Bauer, N., Calvin, K., Dellink, R., Fricko, O., Lutz, W., Popp, A., Cuaresma, J. C., KC, S., Leimbach, M., Jiang, L., Kram, T., Rao, S., Emmerling, J., Ebi, K., Hasegawa, T., Havlik, P., Humpenöder, F., Silva, L. A. D., Smith, S., Stehfest, E., Bosetti, V., Eom, J., Gernaat, D., Masui, T., Rogelj, J., Strefler, J., Drouet, L., Krey, V., Luderer, G., Harmsen, M., Takahashi, K., Baumstark, L., Doelman, J. C., Kainuma, M., Klimont, Z., Marangoni, G., Lotze-Campen, H., Obersteiner, M., Tabeau, A., & Tavoni, M. (2017). The Shared

Socioeconomic Pathways and their energy, land use, and greenhouse gas emissions implications: An overview. *Global Environmental Change*, *42*, 153–168. https://doi.org/10.1016/j.gloenvcha.2016.05.009

Righi, M., Andela, B., Eyring, V., Lauer, A., Predoi, V., **Schlund**, **M.**, Vegas-Regidor, J., Bock, L., Brotz, B., de Mora, L., Diblen, F., Dreyer, L., Drost, N., Earnshaw, P., Hassler, B., Koldunov, N., Little, B., Tomas, S. L., & Zimmermann, K. (2020). Earth System Model Evaluation Tool (ESMValTool) v2.0-technical overview. *Geoscientific Model Development*, *13*(3), 1179–1199. https://doi.org/10.5194/gmd-13-1179-2020

Roe, G. (2009). Feedbacks, Timescales, and Seeing Red. *Annual Review of Earth and Planetary Sciences*, *37*(1), 93–115. https://doi.org/10.1146/annurev.earth.061008.134734

Schlund, **M.**, Lauer, A., Gentine, P., Sherwood, S. C., & Eyring, V. (2020). Emergent constraints on Equilibrium Climate Sensitivity in CMIP5: do they hold for CMIP6? *Earth System Dynamics Discussions*, *2020*, 1–40. https://doi.org/10.5194/esd-2020-49

Schlund, **M.**, Eyring, V., Camps-Valls, G., Friedlingstein, P., Gentine, P., & Reichstein, M. (2020). Constraining Uncertainty in Projected Gross Primary Production With Machine Learning. *Journal of Geophysical Research: Biogeosciences*, *125*(11), e2019JG005619. https://doi.org/10.1029/2019jg005619

Simpkins, G. (2017). Progress in climate modelling. *Nature Climate Change*, *7*(10), 684–685. https://doi.org/10.1038/nclimate3398

Soden, B. J., & Held, I. M. (2006). An Assessment of Climate Feedbacks in Coupled Ocean–Atmosphere Models. *Journal of Climate*, *19*(14), 3354–3360. https://doi.org/10.1175/jcli3799.1

Soden, B. J., Held, I. M., Colman, R., Shell, K. M., Kiehl, J. T., & Shields, C. A. (2008). Quantifying Climate Feedbacks Using Radiative Kernels. *Journal of Climate*, *21*(14), 3504–3520. https://doi.org/10.1175/2007jcli2110.1

Taylor, K. E., Stouffer, R. J., & Meehl, G. A. (2012). An Overview of Cmip5 and the Experiment Design. *Bulletin of the American Meteorological Society*, *93*(4), 485–498. https://doi.org/10.1175/Bams-D-11-00094.1

Vial, J., Dufresne, J. L., & Bony, S. (2013). On the interpretation of inter-model spread in CMIP5 climate sensitivity estimates. *Climate Dynamics*, *41*(11-12), 3339–3362. https://doi.org/10.1007/s00382-013-1725-9

Walker, A. P., De Kauwe, M. G., Bastos, A., Belmecheri, S., Georgiou, K., Keeling, R., McMahon, S. M., Medlyn, B. E., Moore, D. J. P., Norby, R. J., Zaehle, S., Anderson-Teixeira, K. J., Battipaglia, G., Brienen, R. J. W., Cabugao, K. G.,

Cailleret, M., Campbell, E., Canadell, J., Ciais, P., Craig, M. E., Ellsworth, D., Farquhar, G., Fatichi, S., Fisher, J. B., Frank, D., Graven, H., Gu, L., Haverd, V., Heilman, K., Heimann, M., Hungate, B. A., Iversen, C. M., Joos, F., Jiang, M., Keenan, T. F., Knauer, J., Körner, C., Leshyk, V. O., Leuzinger, S., Liu, Y., MacBean, N., Malhi, Y., McVicar, T., Penuelas, J., Pongratz, J., Powell, A. S., Riutta, T., Sabot, M. E. B., Schleucher, J., Sitch, S., Smith, W. K., Sulman, B., Taylor, B., Terrer, C., Torn, M. S., Treseder, K., Trugman, A. T., Trumbore, S. E., van Mantgem, P. J., Voelker, S. L., Whelan, M. E., & Zuidema, P. A. (2020). Integrating the evidence for a terrestrial carbon sink caused by increasing atmospheric CO2. *New Phytologist*, *Accepted Author Manuscript*. https://doi.org/10.1111/nph.16866

WCRP. (2020, November). *WCRP Coupled Model Intercomparison Project (CMIP)*. https://www.wcrp-climate.org/wgcm-cmip

Weigel, K., Bock, L., Gier, B. K., Lauer, A., Righi, M., **Schlund**, **M.**, Adeniyi, K., Andela, B., Arnone, E., Berg, P., Caron, L.-P., Cionni, I., Corti, S., Drost, N., Hunter, A., Lledó, L., Mohr, C. W., Paçal, A., Pérez-Zanón, N., Predoi, V., Sandstad, M., Sillmann, J., Sterl, A., Vegas-Regidor, J., von Hardenberg, J., & Eyring, V. (2020). Earth System Model Evaluation Tool (ESMValTool) v2.0 – diagnostics for extreme events, regional and impact evaluation and analysis of Earth system models in CMIP. *Geoscientific Model Development Discussions*, *in review*, 1–43. https://doi.org/10.5194/gmd-2020-244

Zelinka, M. D., Myers, T. A., Mccoy, D. T., Po-Chedley, S., Caldwell, P. M., Ceppi, P., Klein, S. A., & Taylor, K. E. (2020). Causes of Higher Climate Sensitivity in CMIP6 Models. *Geophysical Research Letters*, *47*(1). https://doi.org/10.1029/2019GL085782

Declaration of Authorship

I assure that this thesis is a result of my personal work and that no other than the indicated aids have been used for its completion. Furthermore I assure that all quotations and statements that have been inferred literally or in a general manner from published or unpublished writings are marked as such. Beyond this I assure that the work has not been used, neither completely nor in parts, to pass any previous examination.

Oberpfaffenhofen, March 2021

Manuel Schlund